Available online at www.sciencedirect.com
ScienceDirect
Advances in Space Research 41 (2008) 396–400
ADVANCES IN SPACE RESEARCH (a COSPAR publication)
www.elsevier.com/locate/asr

INTEGRAL observations of the SNR IC443 region

F. Bocchino [a,*], A.M. Krassilchtchikov [b], P. Kretschmar [c], A.M. Bykov [b], Yu.A. Uvarov [b], S.M. Osipov [b]

[a] *INAF – Osservatorio Astronomico di Palermo, Italy*
[b] *Ioffe Institute of Physics and Technology, St. Petersburg, Russia*
[c] *European Space Astronomy Center, ESA, Villafranca, Spain*

Received 2 November 2006; received in revised form 29 December 2006; accepted 10 January 2007

Abstract

IC433 is a supernova remnant (SNR) interacting with a molecular cloud. The field of IC443 also contains an unidentified gamma-ray source 3EG J0617 + 2238. Recent observations with XMM-Newton and Chandra have revealed a number of hard X-ray sources in the field of the extended SNR including a pulsar wind nebula and an enigmatic hard X-ray source in the SNR – molecular cloud interaction region. We present preliminary results from INTEGRAL observations of IC443. Several sources have been detected by JEM-X, both in the 3–10 and 10–35 keV band, among which is the PWN. We discuss the relation between the JEM-X sources and the detected XMM/Chandra X-ray sources.

Keywords: Supernova remnants: IC443; Non-thermal X-ray emission

1. The supernova remnant IC443

The supernova remnant IC443 is interacting with a neutral cloud in the NE and a molecular cloud in the SE. Signatures of this interactions are evident in the soft X-ray band (Troja et al., 2006) and in the hard X-ray band (Bocchino and Bykov, 2003). A pulsar wind nebula is located inside the remnant (Olbert et al., 2001; Bocchino and Bykov, 2001; Gaensler et al., 2006, Src #5 in Fig. 1). Several compact hard X-ray sources have been identified, mostly located in the region of interaction with the molecular cloud in the SE (marked as numbers in Fig. 1, Bocchino and Bykov, 2003). The brightest of these sources, XMMU J061804.3 + 222732, Src #11 in Fig. 1, has been the subject of additional studies (Bykov et al., 2005), which however did not discriminate between a fast ejecta fragment and a second pulsar wind nebula (associated with the putative overlapping SNR G189.6 + 3.3). We present here new observations of the enigmatic Src #11.

In particular, we present new INTEGRAL observations of the area of the sky containing the SNR IC443 and therefore the Src #11. The 117 science windows (SCWs) used (for a total 420 ks elapsed time) are partly from a long proprietary pointing (PI A. Bykov, AO1) and partly from the Calibration program. We also present here a new XMM-Newton observation of Src #11 carried out on 30.03.2006 (PI F. Bocchino). The exposure time is 60 ks in the PN camera, after screening for intervals affected by proton flares.

We have also used in this work some archive observations. We present a high-resolution optical-to-NIR image of Src #11 (Fig. 5). 2MASS-J and 2MASS-K bands emission of this remnant have been associated with the shock interacting with the neutral cloud and a molecular cloud, respectively (Rho et al., 2001), and therefore it is possible to study the small scale correspondence between X-ray and optical emission of Src #11.

* Corresponding author.
E-mail address: bocchino@astropa.unipa.it (F. Bocchino).

0273-1177/$30
doi:10.1016/j.asr.2007.01.023

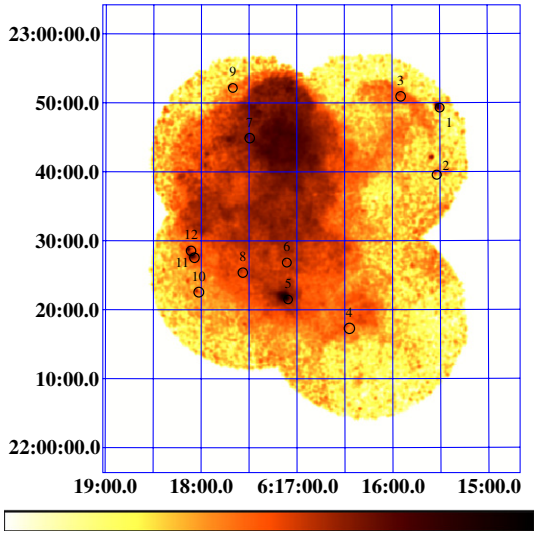

Fig. 1. The hard X-ray emission (1.4–5.0 keV) of the supernova remnant IC443. This is a mosaic of 4 count-rate images obtained from archive XMM-Newton observations of the remnant, background subtracted and vignetting corrected. We have overlaid the location of the 12 hard X-ray sources detected by Bocchino and Bykov (2003) and reported also in the following figures (adapted from Troja et al., submitted for publication).

2. JEM-X images

Unfortunately, the IBIS-ISGRI images of the region are heavily contaminated by ghost sources produced by the Crab nebula, which lies at ~10° distance. For this reason, we have focused ourselves on images from Joint European Monitor for X-rays (JEM-X), which operates simultaneously with the main gamma-ray instruments. JEM-X consists of two identical coded-aperture mask telescopes co-aligned with the other instruments on INTEGRAL . The photon detection system consists of high-pressure imaging Microstrip Gas Chambers (MSGC) located at a distance of 3.4 m from each coded mask. JEM-X is sensitive in the 6–35 keV band and has a spatial resolution of ~3′.

The off-axis angular constraint used in the selection of the observations used in this work was 2.0 degrees in order to avoid the borders of the FOV affected by the poorly known vignetting effect.

In Fig. 2, we show the count-rate image in the 6–20 keV band. We have also computed the significance map. The JEM-X significance is routinely calculated by the standard INTEGRAL reduction software (“OSA”) and it is not a sigma value. A value greater than 12 (corresponding to dark brown color) is considered a reliable detection (JEM-X Analysis Manual, sect. 8.7.1; for further info on this parameter, see Lund et al., 2003; Chernyakova et al., 2005b,a). In Fig. 3 we show the significance map in two bands, 6–10 keV and 10–20 keV. We have tentatively identified the counterparts of Src #5 and Src #11 (marked by arrows). Considering that the positions of the sources on the spatially variable background of JEM-X can be uncertain by a few arc min, the selection of possible counterpart has been made also considering other X-ray properties beyond the XMM position. For example, in the left panel of Fig. 3, we suggest that the JEM-X excess is the counterpart of XMM-Newton Src #5 because Src #8 has an X-ray flux ~10 times below then Src #5 (Bocchino and Bykov, 2003). Moreover, the brighter excess near (6:17:30, 22:35:00.0) in the 6–10 keV image is considered suspicious because in the 15–25 keV band or with RadiusLimit = 100 (the more conservative limit for the “good” detector area) is not seen at all, unlike the counterparts of Src #5 and #11.

In Table 1, we report the measured JEM-X fluxes of the two excesses associated with the XMM-Newton sources, while in Fig. 4 we show their broadband spectra. The fluxes were derived from the images via a cross-calibration with Crab. The errors can be roughly estimated from the JEM-X significances assuming significance = 15 for a 3σ detection. In spite of relatively high value of the JEM-X significance (especially for Src #5), we have chosen to represent the JEM-X fluxes as upper limits in Fig. 4 since we adopted a very conservative choice of the background,

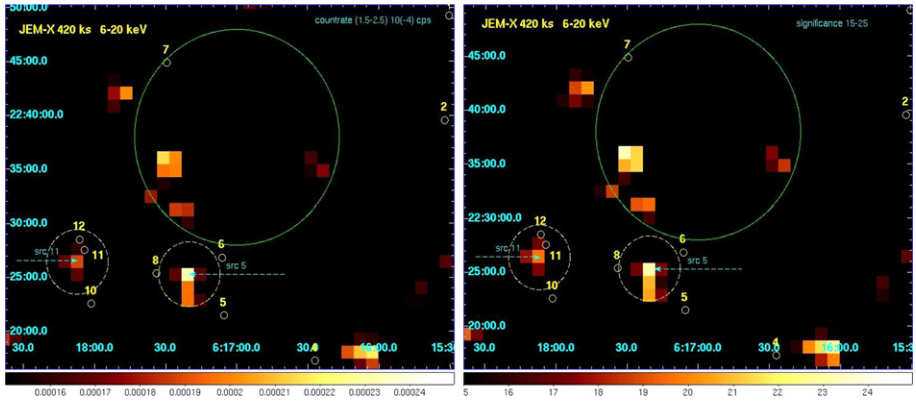

Fig. 2. INTEGRAL JEM-X broadband (6–20 keV) images of the region of IC443 with pixel size of 1.5′. (Left) Count rate map; (right) JEM-X significance map. The positions of the EGRET source and of the 12 sources detected in the XMM observation by Bocchino and Bykov (2003) are also indicated.

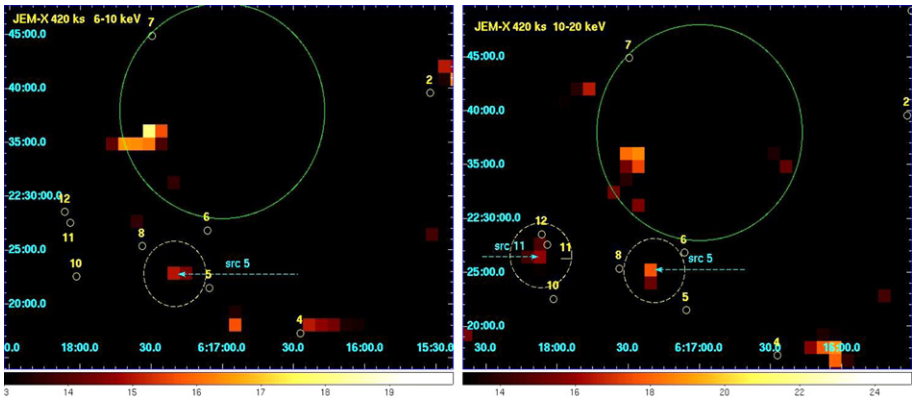

Fig. 3. Same field as Fig. 2, but in two different bands. The images represent JEM-X significance maps in the 6–10 keV and 10–20 keV bands, the linear scale runs from 14 to 20 JEM-X significance units. Tentative identifications are marked with arrows.

Table 1
Fluxes measured by JEM-X for the two possible counterparts of Src #5 (the pulsar wind nebula) and Src #11, indicated with arrows in Fig. 3

Band (keV)	Src #5 (PWN)		Src #11	
	flux (cgs) 10^{-11}	JEM-X Significance	flux (cgs) 10^{-11}	JEM-X Significance
3–10	1.1	21.8	0.7	14.0
6–10	0.5	15.0	0.4	10.7
10–20	1.3	17.6	1.1	15.9
10–35	5.7	29.6	2.1	11.5

which we will improve in a future work. We recall moreover that the JEM-X significance is not the usual statistical σ (see above). The JEM-X upper limits are consistent with the extrapolation of the X-ray spectra of the two XMM-Newton sources (Src #5 and #11), but unfortunately they are not particularly constraining.

We note that both the XMM sources and their JEM-X counterparts are outside the 95% localization circle of the EGRET source 3EG J0617 + 2238. This does not imply necessarily that the sources are not related. In fact, the positional accuracy of relatively faint sources in the Galactic plane has been reported by Gehrels et al. (2001) to be of the order of 1°. In general, therefore, an X-ray with a hard enough spectrum and sufficient energetics to reach the EGRET fluxes that lie within half a degree from the nominal EGRET position could be treated as a possible counterpart for the gamma-ray source. For further detail, see the discussion on the relation between IGR J2018 + 4043 and 3EG J2020 + 4017 in Bykov et al. (2006) and the references therein.

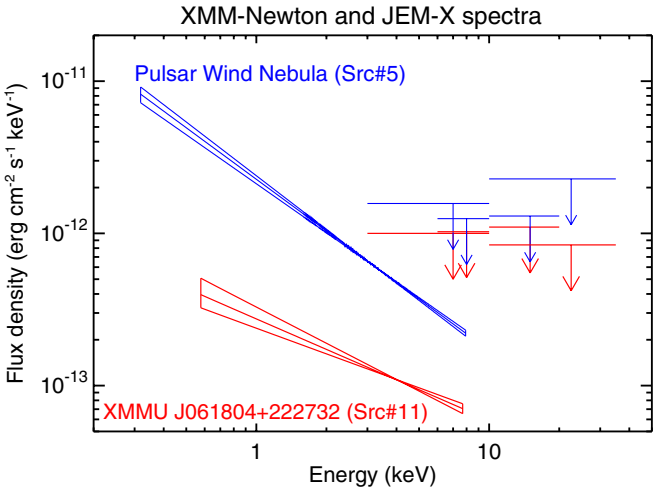

Fig. 4. Broadband spectra of the PWN and Src #11. The JEM-X values are computed from Table 1 and are considered upper limits. The XMM-Newton spectrum is the best-fit model to integrated data of the PWN and Src #11 complex, with errors.

3. Optical/infrared counterparts of Src #11?

Bocchino and Bykov (2003) have noticed that, in general, the hard X-ray sources detected in the SNR IC443 (and showed as numbers on Fig. 2) tend to group together in a small region of the sky (~100 arc min^2) in the south-east of the remnant, nearby a bright large-scale patch of IR emission attributed to the interaction between a radiative shock and a dense molecular cloud.

Here we investigate if this correlation between X-ray and IR also holds at very small spatial scales, around Src #11, which is the brightest hard X-ray source after the PWN. Fig. 5 shows the archive optical and infrared images of the environment of Src #11, as well the position of the X-ray peak identified by Bykov et al. (2005). In the figure, it is clear that possible counterparts include a handful of point sources in the contours and the diffuse emission region visible in the 2MASS-K_s band. The latter is particularly meaningful, since the emission in this band is thought to originate mostly from shocked molecular

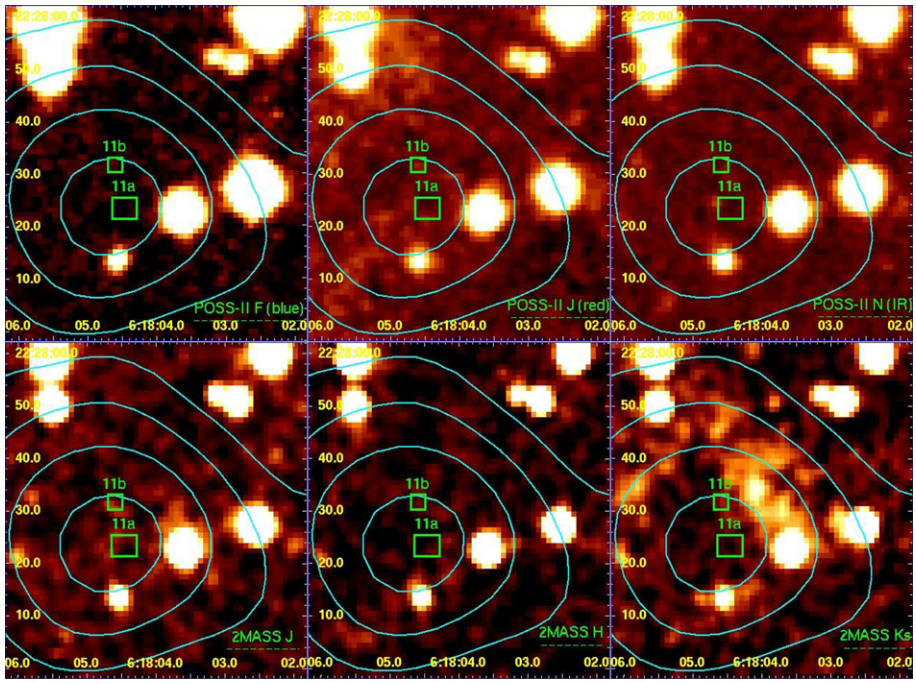

Fig. 5. $1' \times 1'$ field centered on the position of XMM-Newton Src 11. From top-left to bottom right: archive POSS-II images in the blue, red and IR bands. 2MASS archive images with J, H and K_s filters. EPIC 3–8 keV contours of Fig. 6. The positions of the two Chandra X-ray clumps (Src #11a and #11b) discussed by Bykov et al. (2005) are marked with squares, whose size reflects the actual extension of the sources on the Chandra image. Src #12 is outside the field of view. (For interpretation of colours mentioned in the figure legend the reader is referred to the web version of this article.)

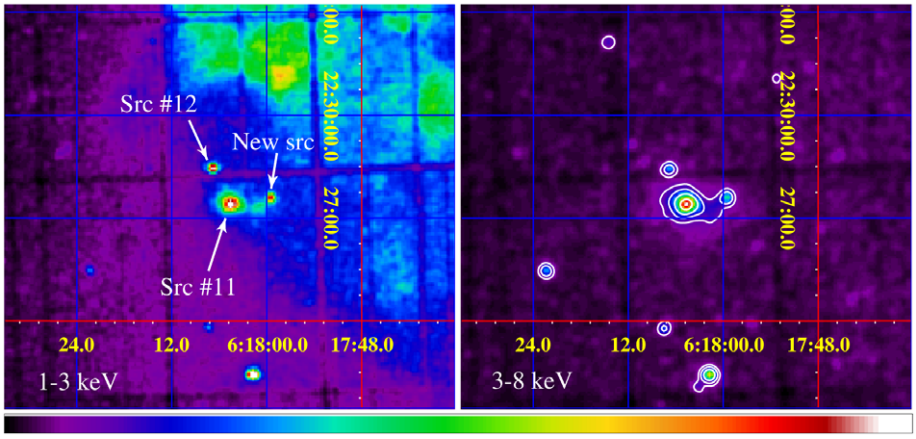

Fig. 6. PN + MOS composite images in 2 different bands of Src #11 reveal a puzzling morphology, with a bridge connecting the main source to a dim source in the west. We have labeled the source names used in the text in the left panel, while we have overlaid the contour levels in the 3–8 keV image (the same contours have been used in Fig. 5).

hydrogen (H_2 $v = 1 - 0$ $S(l)$ line at 2.1 mm, Burton et al., 1988, 1990; Rho et al., 2001).

4. A deeper look in the X-ray morphology of Src #11

The new XMM-Newton observation of Src #11 has revealed an unexpected morphology. In the PN + MOS composite images in 2 different bands shown in Fig. 6, the source is apparently immersed in a large region of diffuse emission. A bright bridge extends between Src #11 and the faint source at the right (labeled "New src"). The bridge and the new source at its right had not been detected in the Chandra observation reported by Bykov et al. (2005), which, instead, has resolved the core of Src #11 into two clumps (Src #11a and #11b shown in Fig. 5), $\sim 8''$ apart.

The full spatial and spectral analysis of the new XMM-Newton data will be reported in a forthcoming paper. In summary, the spectra of the source, the diffuse emission in which it is immersed and the bridge seems to be predominantly non-thermal. In particular, the fit parameters of a region which included all the features around Src #11 are $N_H = 8 \pm 1 \times 10^{21}$ cm^{-2}, $\gamma = 1.7 \pm 0.1$. The fit gives a good description of the data, especially above 2 keV (Fig. 7). At lower energies there is a residual contamination from SNR thermal plasma. The spectral index is suspiciously similar

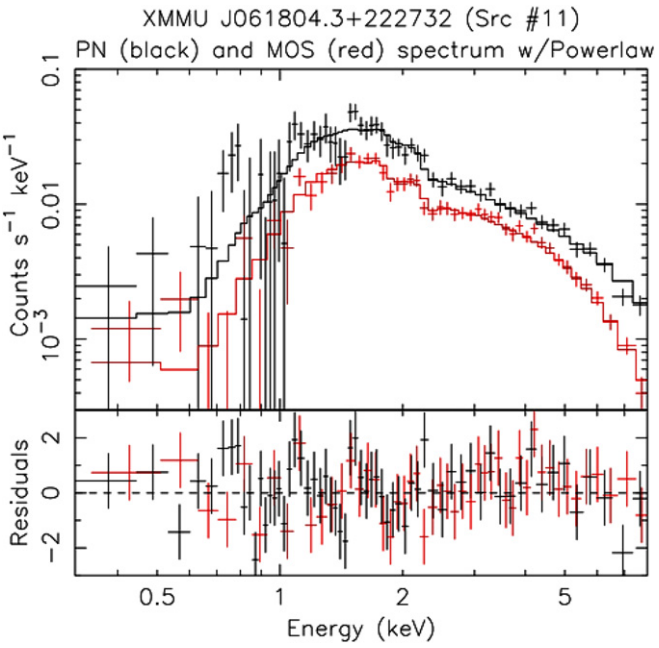

Fig. 7. PN + MOS spectrum of Src #11 (including the bridge and the new source in Fig. 6). The spectrum is fitted with a non-thermal powerlaw (best-fit is also reported).

to that from a background AGN, and we can not yet firmly rule out any of the origins, though it seems unlikely that all the feature observed by Chandra and XMM-Newton in such a small region are AGNs.

5. Discussion and conclusions

A collection of INTEGRAL observation of the region of IC443 has revealed possible counterparts in the hard X-band for the pulsar wind nebula and for the enigmatic source XMMU J061804.3 + 222732 (Src #11), located in a region where interaction between the remnant and a dense molecular cloud is occurring. However, the nature of the Src #11 remains puzzling. We have detected a bridge of extended emission extending toward the faint new source (see Fig. 6), but the nature of the bridge is unknown.

No obvious optical-NIR counterpart is visible on archive observations (Fig. 5). However, the source is located on the inner side of a bright 2MASS-Ks filament which is associated with the shocked molecular cloud, and a small 2MASS-Ks filament located next to the X-ray peak of Src #11 may suggest that Src #11 originates in a dense environment where the interaction between SNR shock and the molecular cloud takes place. One promising interpretation is a fast moving ejecta fragment, whose emission has been modeled by Bykov (2003), and which has been also discussed for IC443 by Bocchino and Bykov (2003) and Bykov et al. (2005). Deep X-ray observations would be very informative to determine the nature of the source, because it may lead to detection of faint X-ray lines emission predicted by the ejecta fragment model.

Acknowledgments

F.B. was supported by a financial contribution from contract ASI-INAF 1/023/05/ The Ioffe team was supported by RBRF Grant 06-02-f 6844.

References

Bocchino, F., Bykov, A.M. The plerion nebula in IC 443: The XMM-Newton view. A&A 376, 248–253, 2001.

Bocchino, F., Bykov, A.M. XMM-Newton study of hard X-ray sources in IC 443. A&A 400, 203–211, 2003.

Burton, M.G., Geballe, T.R., Brand, P.W.J.L., Webster, A.S. Shocked molecular hydrogen in the supernova remnant ic 443. MNRAS 231, 617–634, 1988.

Burton, M.G., Hollenbach, D.J., Haas, M.R., Erickson, E.F. Shocked forbidden O I 63 micron line emission from the supernova remnant IC 443. ApJ 355, 197–209, 1990.

Bykov, A.M. Faint hard X-ray sources in the Galactic Center region: Supernova ejecta fragments population. A&A 410, L5–L8, 2003.

Bykov, A.M., Bocchino, F., Pavlov, G.G. A hard extended X-ray source in the IC 443 supernova remnant resolved by Chandra: a fast ejecta fragment or a new pulsar wind nebula? ApJ 624, L41–L44, 2005.

Bykov, A.M., Krassilchtchikov, A.M., Uvarov, Y.A., Kennea, J.A., Pavlov, G.G., Dubner, G.M., Giacani, E.B., Bloemen, H., Hermsen, W., Kaastra, J., Lebrun, F., Renaud, M., Terrier, R., De Becker, M., Rauw, G., Swings, J.-P. On the Nature of the Hard X-Ray Source IGR J2018 + 4043. ApJ 649, L21–L24, 2006.

Chernyakova, M., Kretschmar, P., Walter, R., Courvoisier, T.-L. JEM-X analysis user manual, vers. 5.1. http://isdc.umge.ch/Soft/download/osa/osa_doc/prod/osaann_jemx-5.1/index.html, 2005a.

Chernyakova, M., Walter, R., Courvoisier, T.-L. Introduction to the INTEGRAL data analysis, vers. 5.1. http://isdc.umge.ch/Soft/download/osa/osa_doc/prod/osa_umJntro-5.1 /index.html, 2005b.

Gaensler, B.M., Chatterjee, S., Slane, P.O., van der Swaluw, E., Camilo, F., Hughes, J.P. The X-ray structure of the pulsar bow shock G189.22 + 2.90 in the supernova remnant IC 443. ApJ 648, 1037–1042, 2006.

Gehrels, N., Macomb, D. J., Bertsch, D. L., Thompson, D. J., Hartman, R. C, Mattson, B. J. Population studies of unidentified 7-ray sources, in: Carraminana, A., Reimer, O., Thompson, D. J. (Eds.), ASSL Vol. 267: The Nature of Unidentified Galactic High-Energy Gamma-Ray Sources, Kluwer Academic Press, Dordrecht, pp. 81–88, 2001.

Lund, N., Budtz-jørgensen, C., Westergaard, N.J., Brandt, S., Rasmussen, I.L., Hornstrup, A., Oxborrow, C.A., Chenevez, J., Jensen, P.A., Laursen, S., Andersen, K.H., Mogensen, P.B., Rasmussen, I., Omø, K., Pedersen, S.M., Polny, J., Andersson, H., Andersson, T., Kamarainen, V., Vilhu, O., Huovelin, J., Maisala, S., Morawski, M., Juchnikowski, G., Costa, E., Feroci, M., Rubini, A., Rapisarda, M., Morelli, E., Carassiti, V., Frontera, F., Pelliciari, C., Loffredo, G., Martinez Nuiiez, S., Reglero, V., Velasco, T., Larsson, S., Svensson, R., Zdziarski, A.A., Castro-Tirado, A., Attina, P., Goria, M., Giulianelli, G., Cordero, F., Rezazad, M., Schmidt, M., Carli, R., Gomez, C., Jensen, P.L., Sarri, G., Tiemon, A., Orr, A., Much, R., Kretschmar, P., Schnopper, H.W. JEM-X: The X-ray monitor aboard INTEGRAL. A&A 411, L231–L238, 2003.

Olbert, C., Clearfield, R.C., Williams, N., Keohane, J., Frail, D.A. ApJ 554, L205, 2001.

Rho, J., Jarrett, T.H., Cutri, R.M., Reach, W.T. Near-infrared imaging and [o i] spectroscopy of ic 443 using two micron all sky survey and infrared space observatory. ApJ 547, 885–898, 2001.

Troja, E., Bocchino, F., Reale, F. XMM-Newton observations of the supernova remnant IC 443. I. Soft X-ray emission from shocked interstellar medium. ApJ 649, 258–267, 2006.

Troja, E., Bocchino, F., Reale, F. XMM-Newton Observations of the Thermal X-ray Emitting Plasma in the Superonva Remnant IC443. Adv. Space Res., submitted for publication.